

See discussions, stats, and author profiles for this publication at: <https://www.researchgate.net/publication/40834995>

Supramolecular Synthesis Based on a Combination of Hydrogen and Halogen Bonds

ARTICLE *in* CRYSTAL GROWTH & DESIGN · JANUARY 2009

Impact Factor: 4.89 · DOI: 10.1021/cg8006712 · Source: PubMed

CITATIONS

64

READS

29

5 AUTHORS, INCLUDING:



Arbin Rajbanshi

Kansas State University

13 PUBLICATIONS 192 CITATIONS

SEE PROFILE

Published in final edited form as:

Cryst Growth Des. 2009 ; 9(1): 432–441. doi:10.1021/cg8006712.

Supramolecular synthesis based on a combination of hydrogen- and halogen bonds

Christer B. Aakeröy^{*,†}, Nate Schultheiss[†], Arbin Rajbanshi[†], John Desper[†], and Curtis Moore

[†]Contribution from the Department of Chemistry, Kansas State University, 111 Willard Hall, Manhattan, Kansas, 66506

[‡]Department of Chemistry, Wichita State University, 1845 Fairmount, Wichita Kansas, 67260

Abstract

A family of supramolecular reagents containing two different binding sites, pyridine and amino-pyrimidine, were allowed to react with iodo- or bromo-substituted benzoic acids in order to assemble individual molecules into larger architectures with precise intermolecular interactions, using a combination of hydrogen- and halogen-bonds. The hydrogen-bond based amino-pyrimidine/carboxylic acid or amino-pyrimidinium/carboxylate synthons are responsible for the assembly of the primary structural motif in every case (7/7 times, 100% supramolecular yield), while $I\cdots N$, $Br\cdots N$, and $I\cdots O$, halogen bonds play a structural supporting role by organizing these supermolecules into extended 1-D and 2-D architectures (5/7 times, 71% supramolecular yield). These results illustrate how two different non-covalent interactions can be employed side-by-side in the reliable construction of extended molecular solid-state networks with predictable connectivity and dimensionality.

Introduction

Successful non-covalent assembly of individual entities into complex heteromeric structures with predetermined connectivities and stoichiometries, which normally relies on a tool-box containing intermolecular interactions such as hydrogen bonds,¹ halogen bonds,² and π - π interactions,³ remains a central challenge within crystal engineering.⁴ Due to the relatively weak and reversible nature of non-covalent intermolecular interactions, the desired product must typically be obtained and isolated in a single-pot reaction, which makes supramolecular synthesis of complex heteromeric targets particularly difficult.⁵

Heteromeric synthons such as carboxylic acid \cdots pyridine,⁶ oxime $\cdots N$ -heterocycles,⁷ and carboxylic acid \cdots amide,⁸ represent useful and versatile supramolecular synthetic tools, Scheme 1. However, although the balance between the two interactions has been explored in homomeric molecular solids⁹, the deliberate combination of different intermolecular interactions such as hydrogen bonds (*e.g.* amino-pyrimidine \cdots carboxylic acid¹⁰) and halogen bonds² has not received as much attention in the assembly of heteromeric molecular solids (co-crystals).¹¹

The synthesis of a specific supermolecular target, such as a heteromeric dimer, can be achieved quite readily if the two different building blocks only contain one binding site each, and if there is only one way in which those two moieties can form a heteromeric synthon. However, synthetic predictability and reliability deteriorates quickly when the number of potentially interacting moieties on each reactant is increased. Several computational approaches have been

developed in order to characterize and quantify the energetic ‘worth’ of multiple intermolecular interactions within a supramolecular system, however it is not necessarily easy to use such information as the basis for practical and transferable *a priori* synthetic strategies for co-crystal synthesis and other supramolecular assembly processes.¹²

A number of systematic structural studies have been performed where hydrogen bonds of different strengths guide and direct the overall assembly of binary and ternary co-crystals in predictable and high-yielding reactions.¹³ However, a strategy for precise synthesis of more complex co-crystals (e.g., quaternary and quinternary) that only relies on hydrogen bonds may soon run into problems because of unavoidable competition between the intended hydrogen-bond donors/acceptors. Therefore, it may be advantageous and, in the long term, more effective to develop supramolecular strategies that can accommodate two different non-covalent interactions in a complementary manner, or in such a way that they are less likely to interfere with each other. A suitable interaction in this context is the halogen bond, which is typically formed between iodine- or bromine atoms (the halogen-bond donor) and an appropriate halogen-bond acceptor (electron-pair donor) such as an *N*-heterocycle. Furthermore, the halogen-bond donor can be boosted substantially by fluorination of the backbone to which the halogen-bond donor is attached, as a result of a dramatic increase in the electron-acceptor ability of the iodine or bromine atom.¹⁴ Since halogen bonds and hydrogen bonds display considerable strength^{2a} and, importantly, directionality, they offer a good starting point for supramolecular strategies that simultaneously encompass two different non-covalent interactions.

In order to utilize the structure-directing abilities of hydrogen bonds and halogens bonds side-by-side we need bifunctional supramolecular reagents (SR's) that contain a robust chemical functionality capable of forming hydrogen bonds even in the presence of other potential disruptive moieties, coupled with a functional group that can facilitate the formation of halogen bonds in a reliable manner. The CSD¹⁵ provides invaluable assistance for identifying suitable compounds that can take advantage of both interactions by minimizing any potential interference between different synthons.

There are ten known crystal structures of co-crystals/salts resulting from the combination of a carboxylic acid and a SR comprising both an amino-pyrimidine and a pyridine moiety. The carboxylic acid preferentially binds to the former site 9/10 times^{10a,16} (equivalent to a 90% supramolecular yield), irrespective of reaction conditions and nature of the carboxylic acid, Scheme 2.

These results clearly demonstrate the robustness of the amino-pyrimidine/carboxylic acid synthon, even in a competitive situation, and we therefore postulated that a pyridine/2-aminopyrimidine-based SR would provide an ideal structure-directing scaffold for constructing supermolecules using assembly-strategies that simultaneously employ hydrogen bonds and halogen bonds. Consequently, by adding a halogen-bond donor (Br or I) to an aromatic carboxylic acid and by allowing it to react with a py/2-aminopyrim SR, we surmised that py···iodine or py···bromine halogen bonds would organize the initial hydrogen-bonded assembly formed *via* carboxylic acid and amino-pyrimidine moieties into extended architectures, Scheme 3.

In order to test our design strategy we synthesized three py/2-aminopyrim SR's, **1–3**, and allowed them to react with either 4-iodobenzoic acid **a**, 2,3,5,6-tetrafluoro-4-iodo-benzoic acid **b**, or 2,3,5,6-tetrafluoro-4-bromo-benzoic acid **c** in a 1:1 ratio, Scheme 4.

We obtained seven crystal structures (from a total of nine reactions), which allowed us to probe whether or not combinations of hydrogen bonds and halogen bonds can be employed in a hierarchical fashion to construct predictable supramolecular assemblies.

Experimental

All chemicals were purchased from Aldrich and used without further purification unless noted. The synthesis and characterization of 3-(2-amino-4-methylpyrimidin-6-yl)pyridine **1**, 4-(2-amino-4-methylpyrimidin-6-yl)pyridine **2**, and 1-(2-amino-4-methylpyrimidin-6-yl)-2-(3-methoxypyridin-5-yl)ethyne **3** are reported elsewhere.^{17,18} 2,3,5,6-Tetrafluoro-4-iodobenzaldehyde and 2,3,5,6-tetrafluoro-4-bromo-benzaldehyde were synthesized following previously published methods.¹⁹ Melting points were determined on a Fisher-Johns melting point apparatus and are uncorrected. Compounds were prepared for infrared spectroscopic (IR) analysis as a mixture in KBr. ¹H NMR spectra were recorded on a Varian Unity plus 200 MHz spectrometer in CDCl₃. Electrospray Ionization – Ion-Trap Mass Spectrometry (ESI-IT-MS) was carried out on a Bruker Daltonics Esquire 3000 Plus.

Synthesis

2,3,5,6-Tetrafluoro-4-iodobenzoic acid, b—A solution of 2,3,5,6-tetrafluoro-4-iodobenzaldehyde (1.52g, 5.20 mmol) in acetone (50 mL) was brought to reflux, when a saturated aqueous solution of KMnO₄ (1.67g, 10.57 mmol) was added. The reaction was heated under reflux for 18h. Upon completion the reaction mixture was filtered hot and the precipitate washed with acetone. The filtrate and the acetone wash were combined and concentrated using a rotary evaporator. The residue was treated with dilute HCl (5 %) and extracted into dichloromethane. The organic layer was washed with water, dried over magnesium sulfate and allowed to evaporate yielding a white solid, 1.29g, 81%. Dec. 140 °C; ¹H NMR (δ_H; 200 MHz, CDCl₃): 8.173 (br s); IR (KBr pellet): ν 2996, 1700, 1475, 979, 718 cm⁻¹; ESI-IT-MS *m/z* 318 ([b - H]⁻).

2,3,5,6-Tetrafluoro-4-bromobenzoic acid, c—A solution of 2,3,5,6-tetrafluoro-4-bromobenzaldehyde (1.54g, 6.29 mmol) in acetone (60 mL) was brought to reflux, when a saturated aqueous solution of KMnO₄ (2.01g, 12.72 mmol) was added. The reaction was kept under reflux for 18h. Upon completion the reaction mixture was filtered hot and the precipitate washed with acetone. The filtrate and the acetone wash were combined and concentrated by rotary evaporator. The residue was treated with dilute HCl (5 %) and extracted into dichloromethane. The organic layer was washed with water, dried over magnesium sulfate and evaporated by rotary evaporator yielding a white solid, 1.32g, 81%. M.p. 128 – 130 °C; ¹H NMR (δ_H; 200 MHz, CDCl₃): 10.16 (br s); IR (KBr pellet): ν 2996, 1711, 1475, 979, 712 cm⁻¹; ESI-IT-MS *m/z* 270 ([c - H]⁻).

Supramolecular synthesis

3-(2-Amino-4-methylpyrimidin-6-yl)pyridine:4-iodobenzoic acid, 1a—3-(2-Amino-4-methylpyrimidin-6-yl)pyridine (10mg, 0.05 mmol) and 4-iodobenzoic acid (13mg, 0.05 mmol) were placed in a beaker containing an ethyl acetate/toluene (2:1) mixture and heated until a clear homogeneous solution was obtained. After two days of slow evaporation, colorless rod-shaped crystals were obtained. M.p. 152–154 °C; IR (KBr pellet) ν 3329 and 3083 cm⁻¹ (NH₂, m), 2413 and 1921 cm⁻¹ (O-H···N, br), 1685 cm⁻¹ (C=O, m).

3-(2-Amino-4-methylpyrimidin-6-yl)pyridine:2,3,5,6-tetrafluoro-4-iodobenzoic acid, 1b—3-(2-Amino-4-methylpyrimidin-6-yl)pyridine (10mg, 0.05 mmol) and 2,3,5,6-tetrafluoro-4-iodobenzoic acid (17mg, 0.05 mmol) were placed in a beaker containing ethanol (6 mL) and heated until a clear homogeneous solution was obtained. After two days of slow

evaporation, colorless rod-shaped crystals were obtained. M.p. 196–198 °C; IR (KBr pellet) ν 3334 and 3104 cm^{-1} (NH_2 , m), 2407 and 1972 cm^{-1} ($\text{O-H}\cdots\text{N}$, br), 1680 cm^{-1} (C=O , m), 963 cm^{-1} (C-I).

4-(2-Amino-4-methylpyrimidin-6-yl)pyridine:4-iodobenzoic acid, 2a—4-(2-Amino-4-methylpyrimidin-6-yl)pyridine (10mg, 0.05 mmol) and 4-iodobenzoic acid (13mg, 0.05 mmol) were placed in a vial containing acetonitrile (6 mL) and heated until a clear homogeneous solution was obtained. After two days of slow evaporation, orange block-shaped crystals were obtained. M.p. 181–183 °C; IR (KBr pellet) ν 3334 and 3176 cm^{-1} (NH_2 , m), 2428 and 1895 cm^{-1} ($\text{O-H}\cdots\text{N}$, br), 1660 cm^{-1} (C=O , m).

4-(2-Amino-4-methylpyrimidin-6-yl)pyridine:2,3,5,6-tetrafluoro-4-iodobenzoic acid, 2b—3-(2-Amino-4-methylpyrimidin-6-yl)pyridine (10mg, 0.05 mmol) and 2,3,5,6-tetrafluoro-4-iodobenzoic acid (17mg, 0.05 mmol) were placed in a vial containing ethanol/ethyl acetate (3:2) and heated until a clear homogeneous solution was obtained. After one day of slow evaporation, colorless rod-shaped crystals were obtained. Dec. 210 °C; IR (KBr pellet) ν 3350 and 2996 cm^{-1} (NH_2 , m), 2387 and 1967 cm^{-1} ($\text{O-H}\cdots\text{N}$, br), 1690 cm^{-1} (C=O , m), 968 cm^{-1} (C-I).

4-(2-Amino-4-methylpyrimidin-6-yl)pyridine:2,3,5,6-tetrafluoro-4-bromobenzoic acid, 2c—3-(2-Amino-4-methylpyrimidin-6-yl)pyridine (10mg, 0.05 mmol) and 2,3,5,6-tetrafluoro-4-bromobenzoic acid (17mg, 0.06 mmol) were placed in a vial containing nitromethane/acetonitrile (5:1) and heated until a clear homogeneous solution was obtained. After one day of slow evaporation, colorless rod-shaped crystals were obtained. M.p. 204–206 °C; IR (KBr pellet) ν 3340 and 3044 cm^{-1} (NH_2 , m), 2361 and 1962 cm^{-1} ($\text{O-H}\cdots\text{N}$, br), 1696 cm^{-1} (C=O , m).

1-(2-Amino-4-methylpyrimidin-6-yl)-2-(3-methoxypyridin-5-yl)ethyne:4-iodobenzoic acid, 3a—1-(2-Amino-4-methylpyrimidin-6-yl)-2-(3-methoxypyridin-5-yl)ethyne (10mg, 0.04 mmol) and 4-iodobenzoic acid (12mg, 0.04 mmol) were placed in a vial containing a methanol/nitromethane solution (2:1) and heated until a clear homogeneous solution was obtained. After four days of slow evaporation, colorless rod-shaped crystals were obtained. M.p. 198–200 °C; IR (KBr pellet) ν 3300 and 3186 cm^{-1} (NH_2 , m), 2478 and 1890 cm^{-1} ($\text{O-H}\cdots\text{N}$, br), 1685 cm^{-1} (C=O , m), 2216 ($\text{C}\equiv\text{C}$, m)

1-(2-Amino-4-methylpyrimidin-6-yl)-2-(3-methoxypyridin-5-yl)ethyne:2,3,5,6-tetrafluoro-4-bromobenzoic acid, 3c—1-(2-Amino-4-methylpyrimidin-6-yl)-2-(3-methoxypyridin-5-yl)ethyne (10mg, 0.04 mmol) and 2,3,5,6-tetrafluoro-4-bromobenzoic acid (12mg, 0.04 mmol) were placed in a vial containing ethanol (6 mL) and heated until a clear homogeneous solution was obtained. After four days of evaporation, colorless rod-shaped crystals were obtained. M.p. 178–180 °C; IR (KBr pellet) ν 3257 and 3186 cm^{-1} (NH_2 , m), 2358 and 1976 cm^{-1} ($\text{O-H}\cdots\text{N}$, br), 1702 cm^{-1} (C=O , m), 2221 ($\text{C}\equiv\text{C}$, m).

X-ray Crystallography

Datasets were collected on a SMART APEX or a SMART 1000 using MoK α radiation and, where noted, were corrected for absorption using the multi-scan procedure implemented by SADABS. Data were collected using SMART.²⁰ Initial cell constants were found by small widely separated “matrix” runs. An entire hemisphere of reciprocal space was collected. Scan speed and scan width were chosen based on scattering power and peak rocking curves. Unit cell constants and orientation matrix were improved by least-squares refinement of reflections thresholded from the entire dataset. Integration was performed with SAINT,²¹ using this improved unit cell as a starting point. Unit cell constants were calculated in SAINT from the

final merged dataset. Lorenz and polarization corrections were applied, and data were corrected for absorption. Data were reduced with SHELXTL.²² The structures were solved by direct methods. Unless otherwise noted, hydrogen atoms were assigned to idealized positions and were allowed to ride. All non-hydrogen atoms were given anisotropic thermal parameters.

1a Data were collected on a SMART APEX at $-120\text{ }^{\circ}\text{C}$. Coordinates of the amine hydrogens H12A and H12B and carboxylic acid hydrogen H31 were allowed to refine. **1b** Data were collected on a SMART 1000 at $-100\text{ }^{\circ}\text{C}$. **2a** Data were collected on a SMART APEX at $-120\text{ }^{\circ}\text{C}$. **2b** Data were collected on a SMART APEX at $-120\text{ }^{\circ}\text{C}$. Proton transfer from acid to amine was clearly observed, and the coordinates of the ammonium hydrogen H11 and amine hydrogens H12A and H12B were allowed to refine. **2c** Data were collected on a SMART APEX at $-120\text{ }^{\circ}\text{C}$. Proton transfer from acid to amine was clearly observed, and the coordinates of the ammonium hydrogen H11 were allowed to refine. **3a** Data were collected on a SMART APEX at $-120\text{ }^{\circ}\text{C}$. Coordinates of the carboxylic acid hydrogen H31 were allowed to refine. **3c** Data were collected on a SMART APEX at $-120\text{ }^{\circ}\text{C}$. Proton transfer from acid to amine was clearly observed, and the coordinates of the ammonium hydrogen H11 and amine hydrogens H12A and H12B were allowed to refine.

Results

SR's **1–3** was synthesized through conventional palladium-catalyzed cross-coupling conditions, while halogenated benzoic acids **b** and **c** were generated in good yields ($\sim 81\%$) from the corresponding halogenated benzaldehydes by conventional oxidation with potassium permanganate. SR's **1–3** were allowed to react with halogenated benzoic acids **a–c** in a 1:1 ratio resulting in seven 1:1 crystalline materials suitable for analysis by single-crystal X-ray diffraction.

The primary motif in the crystal structure of **1a** is an SR:acid dimer assembled *via* a complementary hydrogen-bond interaction between the carboxylic acid and the amino-pyrimidine moiety (there is also one molecule of toluene in the lattice). The primary hydrogen bonds are $\text{O}\cdots\text{H}\cdots\text{N}$ and $\text{N}\cdots\text{H}\cdots\text{O}$ interactions with $\text{O31}\cdots\text{N11}$ and $\text{N12}\cdots\text{O32}$ distances of $2.5607(19)\text{ \AA}$ and $3.035(2)\text{ \AA}$, respectively. Secondary $\text{N}\cdots\text{H}\cdots\text{N}$ hydrogen bonds, $\text{N12}\cdots\text{N21}$, $2.951(2)\text{ \AA}$, between the *anti*-amino proton and the pyridyl nitrogen atom lead to a four-component supermolecule, Figure 2. No structure-directing $\text{I}\cdots\text{N}$ or $\text{I}\cdots\text{I}$ interactions were observed.

In the crystal structure of **1b** the main motif consists of py-pym **1** and 2,3,5,6-tetrafluoro-4-iodobenzoic acid **b** in a 1:1 ratio; the two molecules are connected through the carboxylic acid and amino-pyrimidine moieties *via* $\text{O}\cdots\text{H}\cdots\text{N}$ and $\text{N}\cdots\text{H}\cdots\text{O}$ hydrogen bonds with $\text{O31}\cdots\text{N11}$ and $\text{N12}\cdots\text{O32}$ distances of $2.589(7)\text{ \AA}$ and $2.924(8)\text{ \AA}$, respectively. A halogen bond between the iodine atom and the pyridyl nitrogen atom connects the dimers into 1-D chains, $r(\text{I}\cdots\text{N}_{(\text{py})})\text{ }2.941\text{ \AA}$, $\angle(\text{C-I-N})\text{ }170.7^{\circ}$, Figure 3.

The 1-D chains are connected into a 2-D wave-like pattern through additional $\text{N}\cdots\text{H}\cdots\text{O}$ interactions, $\text{N12}\cdots\text{O32}$, $2.855(8)\text{ \AA}$, involving the *anti*-amino proton and the carbonyl oxygen atom of the benzoic acid, Figure 4.

The crystal structure of **2a** contains dimeric units of SR **2** and 4-iodobenzoic acid, assembled by the carboxylic acid/amino-pyrimidine synthon with $\text{O31}\cdots\text{N11}$ and $\text{N12}\cdots\text{O32}$ distances of $2.675(3)\text{ \AA}$ and $2.818(4)\text{ \AA}$, respectively. An $\text{I}\cdots\text{N}_{(\text{py})}$ halogen bond links dimers into 1-D chains, $r(\text{I}\cdots\text{N})\text{ }3.004\text{ \AA}$, $\angle(\text{C-I-N})\text{ }178^{\circ}$, and adjacent anti-parallel chains are arranged into ribbons through pairs of symmetry related $\text{N}\cdots\text{H}\cdots\text{N}$ hydrogen bonds, $r(\text{N12}\cdots\text{N13})\text{ }2.250\text{ \AA}$, Figure 5.

The primary motif in the crystal structure of **2b** comprises an ion pair of protonated SR **2** and 2,3,5,6-tetrafluoro-4-iodobenzoate ions, interlinked through charge-assisted hydrogen bonds between the carboxylate and amino-pyrimidinium moieties. The primary hydrogen bonds are $\text{N-H}^+\cdots\text{O}^-$ and $\text{N-H}\cdots\text{O}^-$ interactions with $\text{N11}\cdots\text{O31}$ and $\text{N12}\cdots\text{O32}$ distances of 2.646(5) and 2.801(5) Å, respectively. An $\text{I}\cdots\text{N}_{(\text{py})}$ halogen bond connect dimers into 1-D chains, $r(\text{I}\cdots\text{N})$ 2.812 Å, $\angle(\text{C-I-N})$ 177°. The linear chains are linked into a ladder-motif through secondary $\text{N-H}\cdots\text{O}^-$ hydrogen bonds ($\text{N12}\cdots\text{O32}$, 2.808(5) Å), from the *anti*-ammonium proton and the carboxylate oxygen atom, Figure 6.

In the crystal structure of **2c**, one protonated SR **2** and one 2,3,5,6-tetrafluoro-4-bromobenzoate ion, form produce a charge-assisted hydrogen-bonds between the carboxylate and the amino-pyrimidinium moieties, Figure 7, with $\text{N-H}^+\cdots\text{O}^-$ and $\text{N-H}\cdots\text{O}^-$ distances of ($\text{N11}\cdots\text{O32}$, 2.6430(19) Å) and ($\text{N}^+12\cdots\text{O32}$, 2.823(2) Å), respectively. A halogen bond between ion-pairs produces an infinite 1-D chain, $r(\text{Br}\cdots\text{N}_{(\text{py})})$ 2.840 Å, $\angle(\text{C-Br-N})$ 177°, while the *anti*-proton of the amino group forms a charge-assisted $\text{N-H}\cdots\text{O}^-$ hydrogen bond ($\text{N12}\cdots\text{O32}$, 2.812(2) Å) with a neighboring carboxylate oxygen atom.

The primary motif in the crystal structure of **3a** is constructed through $\text{O-H}\cdots\text{N}$ and $\text{N-H}\cdots\text{O}$ interactions with $\text{O31}\cdots\text{N11}$ and $\text{N12}\cdots\text{O32}$ distances of 2.643(8) Å and 2.987(8) Å, respectively. An $\text{O}_{(\text{methoxy})}\cdots\text{I}$ halogen bond ($r(\text{O}\cdots\text{I})$ 3.265 Å, $\angle(\text{C-I-O})$ 178°) produces an infinite chain, while the *anti*-proton of the amino group forms an $\text{N-H}\cdots\text{N}$ hydrogen bond ($\text{N12}\cdots\text{N13}$, 3.108(8) Å) with a pyrimidine nitrogen atom of a neighboring strand generating a ladder motif, Figure 8.

The crystal structure of **3c** contains an ion-pair comprising one protonated SR **3** and one 2,3,5,6-tetrafluoro-4-bromobenzoate ion, held together *via* charge assisted hydrogen bonds, Figure 9. Proton transfer occurs from the carboxylic acid to the pyrimidine nitrogen atom, with $\text{N11}\cdots\text{O31}$ and $\text{N12}\cdots\text{O32}$ distances of 2.605(2) Å and 2.832(2) Å, respectively. Adjacent ion-pairs are connected through self-complementary $\text{N-H}\cdots\text{N}$ hydrogen bonds, ($\text{N12}\cdots\text{N13}$) 3.073(2) Å, producing a four-component aggregate, Figure 9. No short $\text{Br}\cdots\text{N}$ or $\text{Br}\cdots\text{Br}$ interactions are present.

Discussion

It is possible that a wide variety of intermolecular interactions and supramolecular products could result from the reaction between a pyridine/aminopyrimidine-based SR and a carboxylic acid/halogen-bond donor based-molecule, especially since many of the plausible hetero- and/or homomeric synthons are already well-known in crystal engineering, Scheme 5.

However, despite this potential structural ‘chaos’, the overall result is remarkably consistent because in each of the seven cases, the carboxylic binds to the aminopyrimidine site instead of to the pyridyl moiety (even though the latter is a very capable hydrogen-bond acceptor). Although proton transfer does take place in three of the seven structures, **2b**, **2c**, and **3c**, the charge-assisted $\text{N-H}^+\cdots\text{O}^-$ and $\text{N-H}\cdots\text{O}^-$ synthon is a mimic of the neutral analogue, and does not interfere with the intended assembly. Furthermore, the presence of a carboxylate moiety does not introduce any additional components in these cases.²³ $\text{I}\cdots\text{N}$, $\text{Br}\cdots\text{N}$, or $\text{I}\cdots\text{O}$ halogen bonds were observed in five of the seven structures (71% supramolecular yield), **1b**, **2a–2c**, and **3a** resulting in extended 1-D or 2-D networks, Table 3.

In each case **1b** and **2a–2c** halogen bonding occurs with $\text{X}\cdots\text{N}$ ($\text{X} = \text{I}, \text{Br}$) distances ranging from 2.812 – 3.004 Å, which are considerably shorter than the sum of the van der Waals radii for nitrogen (1.55 Å) and iodine (1.98 Å) or bromine (1.85 Å).²⁴ The $\text{I}\cdots\text{O}$ distance (3.265 Å) found in structure **3a** is also within the overall sum of the van der Waals radii for oxygen and

iodine (3.53 Å). Furthermore, C-X \cdots N angles near linear 170.7–178.1 Å indicate significant (n- σ^*) charge-transfer character.^{2a, 25}

It has been determined experimentally and computationally that halogen bond strength decreases in the order I > Br > Cl with various Lewis bases.²⁶ However, due to the limited number of structures within our study, it is difficult to draw precise conclusions about the relative ability of iodine or bromine atoms to act as halogen-bond donors when interacting with a N-containing heterocycle. Thus, to compare the supramolecular reactivity of bromine or iodine and a N-heterocycle, we complemented our results with relevant structural data from the CSD, Table 4.²⁷

Forty structures were found containing short Br \cdots N interactions, and eleven of those involved fluorinated (“activated”) organic bromine. In comparison, sixty-two structures were found containing short I \cdots N contacts; both fluorinated (41/62) and non-fluorinated (21/62) organic iodine can drive the supramolecular assembly. This analysis offers further indication that the iodine atom is a superior halogen-bond donor compared to a bromine atom when a nitrogen-containing heterocycle is employed as the halogen-bond acceptor.²⁸

We attempted to determine if an increase in Lewis acidity, due to fluorination around the halogen nuclei (-I or -Br) proves advantageous in forming stronger (based on X \cdots N distances) halogen bonds. The molecules in structure **2b** display a shorter I \cdots N distance, 2.812 Å, in comparison to **2c**, which has an Br \cdots N distance of 2.840 Å, even though an iodine atom (1.32 Å) is larger than a bromine atom (1.14 Å). As expected, comparing structures **2a** and **2c**, the halogen bond distance becomes shorter upon fluorination of the aryl ring (3.004 Å vs. 2.812 Å). Furthermore, fluorinated iodo-benzoic acid produces both hydrogen and halogen bonds when combined with **1**, whereas the reaction between 4-iodo benzoic acid and **1** did not yield any halogen bonds. These results are consistent with the fact that organic iodine is a stronger Lewis acid than the corresponding bromine species. Furthermore, fluorination of the carbon backbone of the halogen atom increases the structural influence of this halogen-bond donor as a result of an increase in Lewis acidity.

Herein we have described a strategy for designing and constructing supermolecules through combinations of hydrogen bonds and halogen bonds. In all seven structures the carboxylic acid \cdots amino-pyrimidine or carboxylate \cdots amino-pyrimidinium synthon was present and served to ‘lock’ the two discrete molecules (or ions) into a well-defined dimer. The fact that this synthon was present in each case, means that it can be designated as the primary (and structure directing) intermolecular interaction in this series of compounds. In five of the seven crystal structures, the primary dimers were subsequently organized into infinite 1-D chains through I \cdots N or Br \cdots N halogen bonds (4/5), and I \cdots O halogen bonds (1/2). Intermolecular distances in these seven structures consistently support the expected behavior based upon changes in Lewis acidity of fluorinated/non-fluorinated organic iodine/bromine halogen-bond donor sites.

The relative supramolecular yields of the hydrogen-bond and halogen-bond based synthons, translate into a hierarchy of structural influence that can form the basis for new strategies for the directed assembly of more complex, multimeric, molecular architectures.

Acknowledgments

We are grateful for the financial support from ACS-PRF (46011-AC1), the Terry C. Johnson Center for Basic Cancer Research, and for a Grant (P20 RR015563) from the National Center for Research Resources, a component of the National Institutes of Health, and the State of Kansas. This manuscript is solely the responsibility of the authors and does not necessarily represent the official view of the NCRR or NIH.

References

1. (a) Aakeröy CB, Salmon DJ. *CrystEngComm* 2005;7:439. (b) MacGillivray L. *CrystEngComm* 2004;6:77. (c) Lehn J-M. *Science* 2002;295:2400. [PubMed: 11923524] (d) Desiraju GR. *Acc. Chem. Res* 2002;35:565. [PubMed: 12118996] (e) Moulton B, Zaworotko MJ. *Chem. Rev* 2001;101:1629. [PubMed: 11709994] (f) Desiraju GR. *Angew. Chem., Int. Ed. Engl* 1995;34:2311. (g) Wenger M, Bernstein J. *Angew. Chem. Int. Ed* 2006;45:7966. (h) Childs SL, Hardcastle KI. *CrystEngComm* 2007;9:364. (i) Bosch E. *CrystEngComm* 2007;9:191.
2. (a) Metrangolo P, Neukirch H, Pilati T, Resnati G. *Acc. Chem. Res* 2005;38:386. [PubMed: 15895976] (b) Metrangolo P, Pilati T, Resnati G, Stevenazzi A. *Chem. Commun* 2004:1492. (c) De Santis A, Forni A, Liantonio R, Metrangolo P, Pilati T, Resnati G. *Chem. Eur. J* 2003;9:3974. (d) Walsh RB, Padgett CW, Metrangolo P, Resnati G, Hanks TW, Pennington WT. *Cryst. Growth Des* 2001;1:165. (e) Cincic D, Friscic T, Jones W. *J. Am. Chem. Soc* 2008;130:7524. [PubMed: 18491900] (f) Cincic D, Friscic T, Jones W. *Chemistry—A Eur. J* 2008;14:747. (g) Shirman T, Freeman D, Posner YD, Feldman I, Facchetti A, van der Boom ME. *J. Am. Chem. Soc* 2008;130:8162–8163. [PubMed: 18529052] (h) Nguyen HL, Horton PN, Hursthouse MB, Legon AC, Bruce DW. *J. Am. Chem. Soc* 2004;126:16–17. [PubMed: 14709037] (i) Triguero S, Llusar R, Polo V, Fourmigué M. *Cryst. Growth Des* 2008;8:2241–2247. (j) Meyer EA, Castellano RK, Diederich F. *Angew. Chem. Int. Ed* 2003;42:1210.
3. (a) Barooah N, Sarma RJ, Baruah JB. *CrystEngComm* 2006;8:608. (b) Motohiro N. *CrystEngComm* 2004;6:130.
4. (a) Grepioni, F.; Braga, D. *Making Crystals by Design - from molecules to molecular materials, methods, techniques, applications*. Wiley-VCH: 2007. (b) Steed, JW.; Atwood, JL. *Supramolecular Chemistry*. Chichester: John Wiley & Sons: Ltd; 2000. (c) Desiraju, GR. *The Crystal as a Supramolecular Entity*. New York: John Wiley & Sons: Ltd; 1996. (d) Lehn, J-M. *Supramolecular chemistry: concepts and perspectives*. Weinheim: VCH; 1995.
5. Aakeröy CB, Beatty AM, Helfrich BA. *Angew. Chem. Int Ed* 2001;40:3240.
6. (a) Mei X, Wolf C. *Eur. J. Org. Chem* 2004:4340. (b) Dale SH, Elsegood MRJ, Hemmings M, Wilkinson AL. *CrystEngComm* 2004;6:207. (c) Bhogala BR, Nangia A. *Cryst. Growth Desn* 2003;3:547. (d) Bensemann I, Gdaniec M, Lakomecka K, Milewska MJ, Polonski T. *Org. Biomol. Chem* 2003;1:1425. [PubMed: 12929674] (e) Hguyen TL, Fowler FW, Lauher JW. *J. Am. Chem. Soc* 2001;123:11057. [PubMed: 11686712]
7. Aakeröy CB, Salmon DJ, Smith MM, Desper J. *Cryst. Growth Des* 2006;4:1033.
8. (a) Vishweshwar P, McMahon JA, Peterson ML, Hickey MB, Shattock TR, Zaworotko MJ. *Chem. Commun* 2005;36:4601. (b) Aakeröy CB, Desper J, Helfrich BA. *CrystEngComm* 2004;6:19. (c) Reddy LS, Nangia A, Lynch VM. *Cryst. Growth Desn* 2004;4:89. (d) Aakeröy CB, Beatty AM, Helfrich BA, Nieuwenhuyzen M. *Cryst. Growth Des* 2003;3:159. (e) Ito Y, Hosomi H, Ohba S. *Tetrahedron* 2000;56:6833.
9. (a) Saha BK, Nangia A, Jaskólski M. *CrystEngComm* 2005;7:355. (b) George S, Nangia A, Lam C-K, Mak TCW, Nicoud J-F. *Chem. Commun* 2004:1202. Reddy LS, Chandran SK, George S, Babu NJ, Nangia A. *Cryst. Growth. Des* 2007;12:2675.
10. (a) Aakeröy CB, Schultheiss N, Desper J, Moore C. *New J. Chem* 2006;30:1452. (b) Thanigaimani K, Muthiah PT, Lynch DE. *Acta Cryst* 2006;E62:2976. (c) Balasubramani K, Muthiah PT, Lynch DE. *Acta Cryst* 2006;E62:2907. (d) Smith G, Gentner JM, Lynch DE, Byriel KA, Kennard CHL. *Aust. J. Chem* 1995;48:1151. (e) Etter MC, Adsmond DA. *Chem. Commun* 1990:589.
11. (a) Aakeröy CB, Fasulo M, Schultheiss N, Desper J, Moore C. *J. Am. Chem. Soc* 2007;129:13772. [PubMed: 17956090] Aakeröy CB, Desper J, Helfrich BA, Metrangolo P, Pilati T, Resnati G, Stevenazzi A. *Chem. Commun* 2007:4236. Bouchmella K, Boury B, Dutremez SG, van der Lee A. *Chem.-Eur. J* 2007;13:6130. Goroff NS, Curtis SM, Webb JA, Fowler FW, Lauher JW. *Org. Lett* 2005;7:1891. [PubMed: 15876012]
12. (a) Dunitz JD, Gavezzotti A. *Angew Chem. Int. Ed* 2005;44:1766. (b) Brandhost K, Grunenberg J. *ChemPhysChem* 2007;8:1151. [PubMed: 17477339] (c) Putz MV. *Advances in Quantum Chemical Bonding*. 2008

13. (a) Aakerøy CB, Desper J, Smith MM. Chem. Commun 2007;38:3936. (b) Aakerøy CB, Desper J, Scott BMT. Chem. Commun 2006;13:1445. (c) Aakerøy CB, Desper J, Urbina JF. Chem. Commun 2005;22:2820.
14. Metrangolo, P.; Resnati, G., editors. Structure and Bonding Vol. 126. Halogen bonding: fundamentals and applications. Berlin: Springer; 2008.
15. Allen FH. Acta Cryst 2002;B58:380–388.
16. Lynch DE, McClenaghan I. Acta Cryst 2001;C57:830.
17. Aakerøy CB, Schultheiss N, Desper J. Inorg. Chem 2005;44:4983. [PubMed: 15998026]
18. Aakerøy CB, Schultheiss N, Desper J, Moore C. Cryst. Growth Des 2007;7:2324.
19. (a) Leroy J, Schollhorn B, Syssa-Magale J-L, Boubekeur K, Palvadeau P. J. Fluorine Chem 2004;125:1379. (b) Krebs FC, Jensen T. J. Fluorine Chem 2003;120:77. (c) Robson, MJ.; Williams, J. European Patent. #EP 0 196 156 B1. 1986.
20. SMART v5.060. © 1997 – 1999, Bruker Analytical X-ray Systems. Madison, WI:
21. SAINT v6.02. © 1997 – 1999, Bruker Analytical X-ray Systems. Madison, WI:
22. SHELXTL v5.10. © 1997, Bruker Analytical X-ray Systems. Madison, WI:
23. Aakerøy CB, Fasulo ME, Desper J. Molecular Pharm 2007;4:317.
24. Bondi A. J. Phys. Chem 1964;68:441.
25. Rosokha SV, Neretin IS, Rosokha TY, Hecht J, Kochi JK. Heteroatom Chem 2006;17:449.
26. (a) Guardigli C, Liantoni R, Mele ML, Metrangolo P, Resnati G, Pilati T. Supramol. Chem 2003;15:177. (b) Politzer P, Lane p, Concha MC, Ma Y, Murray JS. J. Mol. Model 2007;13:305. [PubMed: 17013631] (c) Lommerse JPM, Stone AJ, Taylor R, Allen FH. J. Am. Chem. Soc 1996;118:3108.
27. ConQuest, version 5.28. Cambridge, U.K: Cambridge Structural Database; . A typical search was based upon defining the inter-molecular contact $X \cdots N$ ($X = I$ or Br) using the distance within the sum of the VdW radii + 0.0 Å. Search criterion included only organics, no ions and an $R < 0.05$.
28. Metrangolo P, Meyer F, Pilati T, Resnati G, Terraneo GA. Angew. Chem. Int. Ed 2008;47:6114. Metrangolo P, Resnati G. Science 2008;321:918. [PubMed: 18703728]

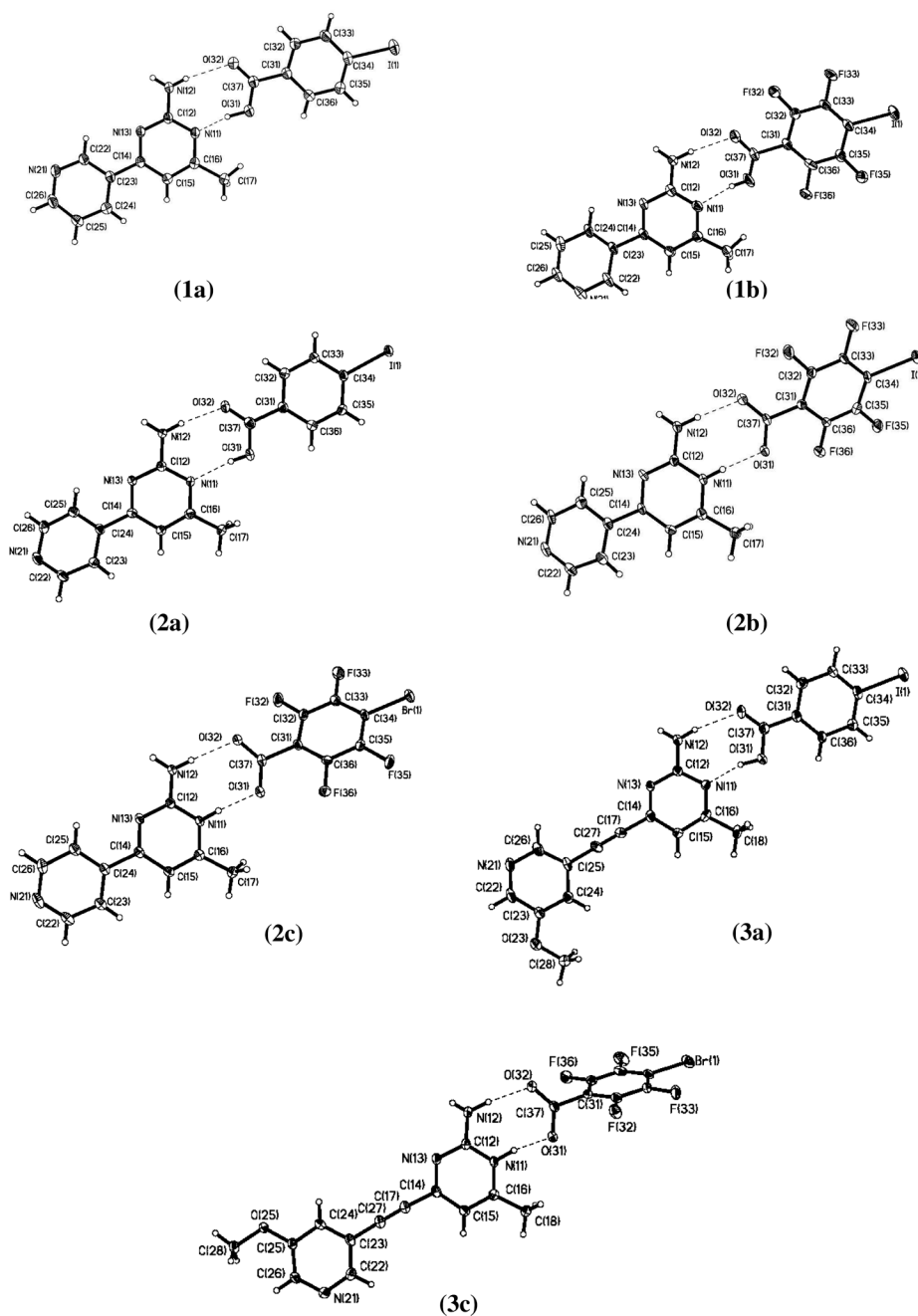


Figure 1.
Labeled thermal-ellipsoid plots (50% probability level) of **1a–1b**, **2a–2c**, **3a**, and **3c**.

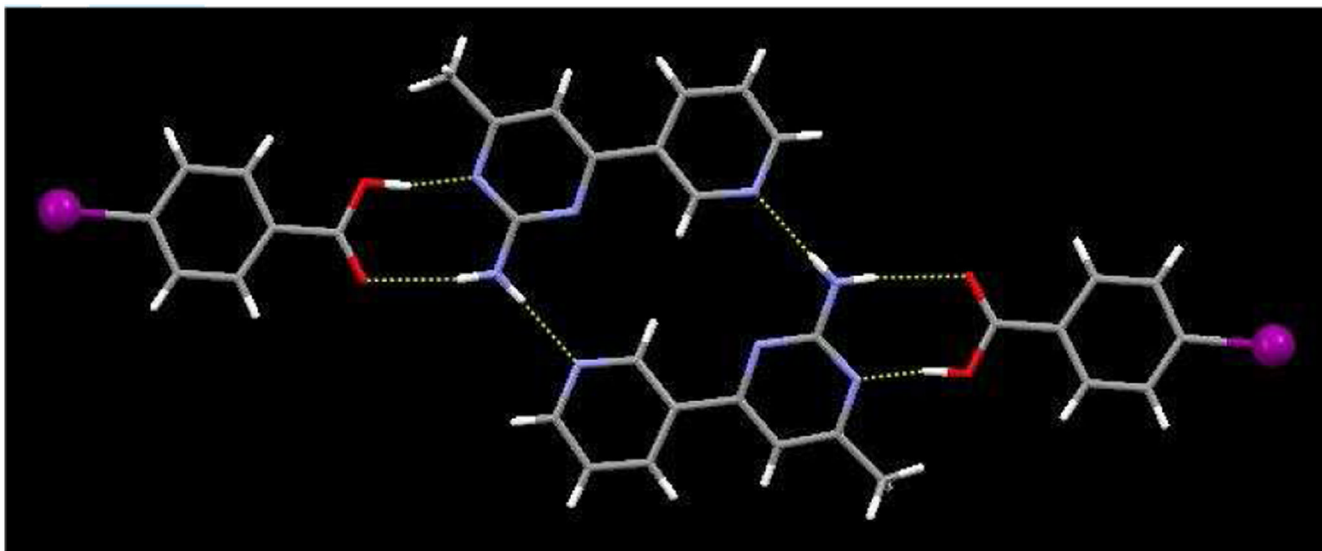


Figure 2.

Four-component supermolecule in **1a** comprised of N-H \cdots O, O-H \cdots N, and N-H \cdots N hydrogen bonds. The toluene solvent molecule has been omitted for clarity.

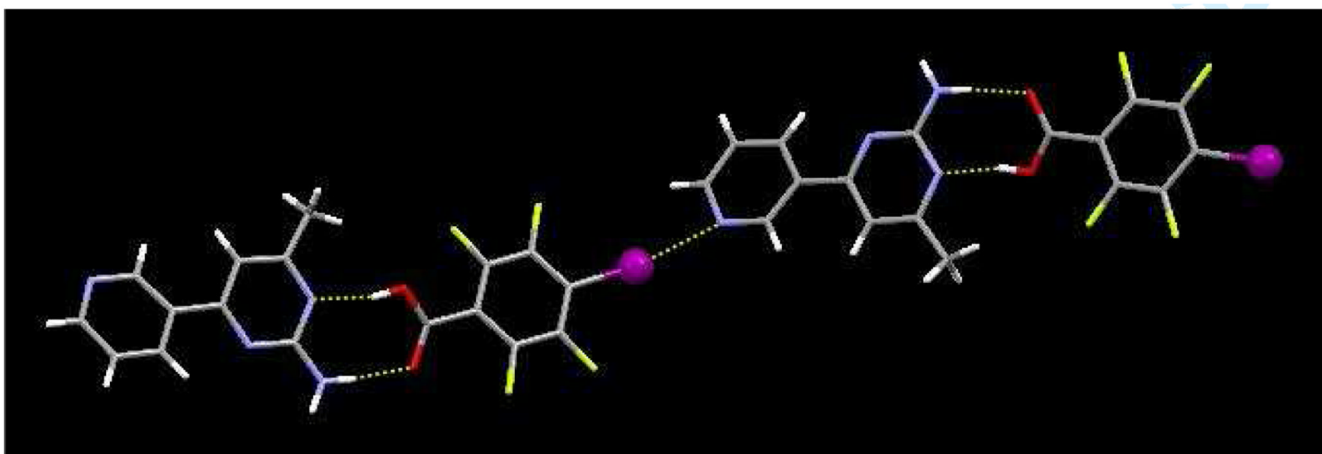


Figure 3.
1-D chain in **1b**, generated through amino-pyrimidine...acid and I...N synthons.

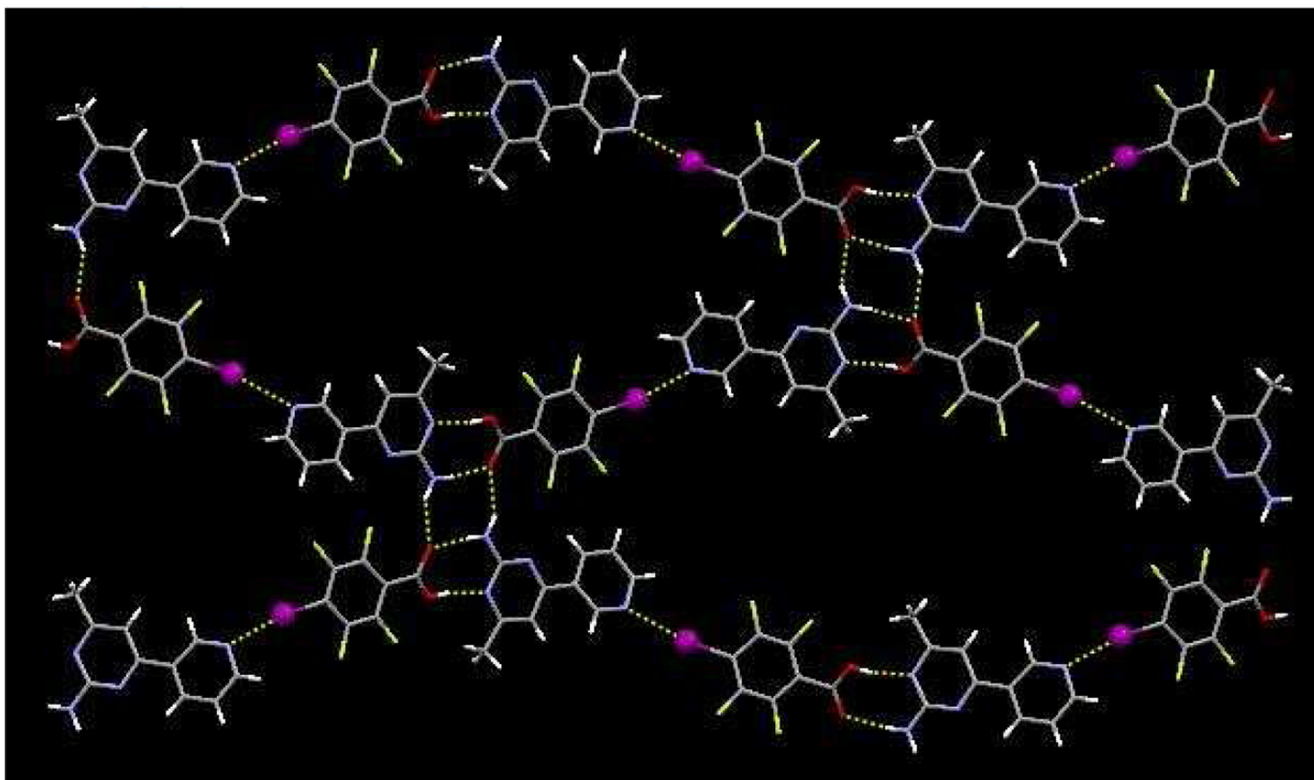


Figure 4.
Extended motif of **1b**, displaying a sheet constructed from O–H...N, N–H...O hydrogen bonds and I...N halogen bonds.

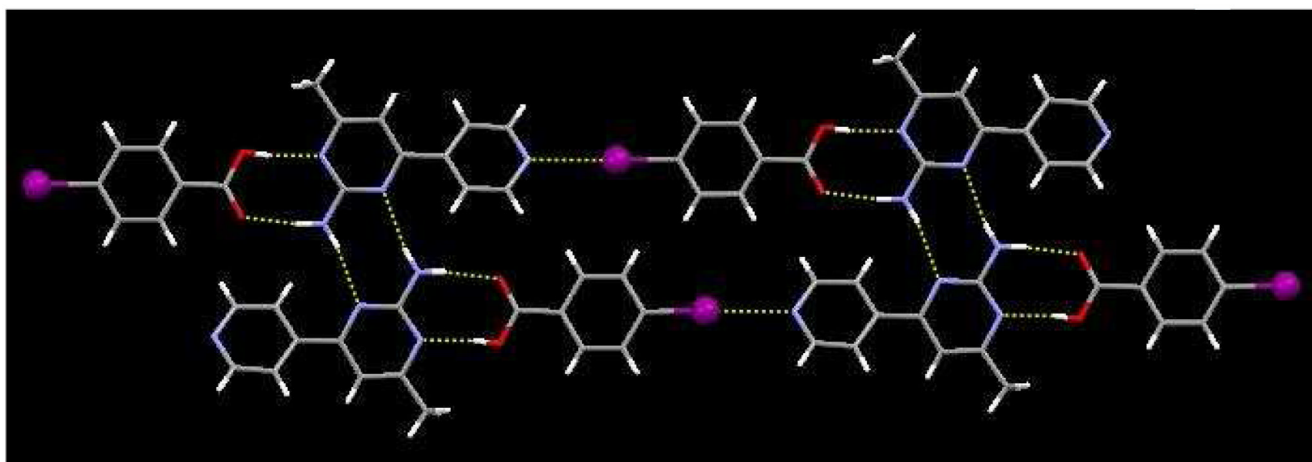


Figure 5.
Ladders in the structure of **2a** constructed from a combination of O–H···N, N–H···O, and N–H···N hydrogen bonds and I···N halogen bonds.

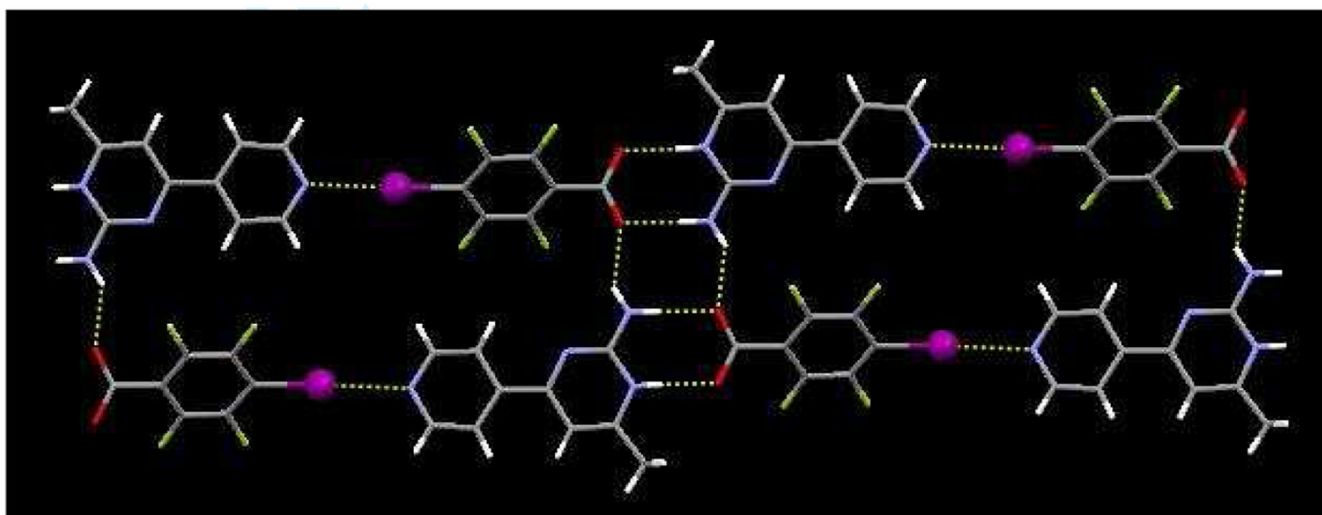


Figure 6.
1-D strands in **2b** formed through a series of hydrogen bonds and halogen bonds.

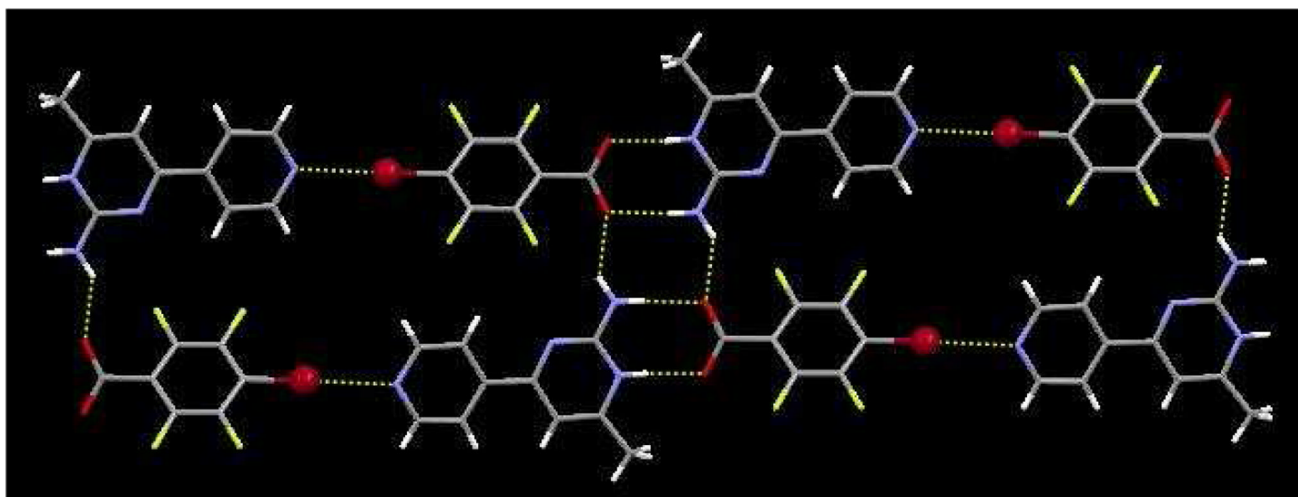


Figure 7.
1-D strands in **2c** formed through a series of hydrogen bonds and halogen bonds.

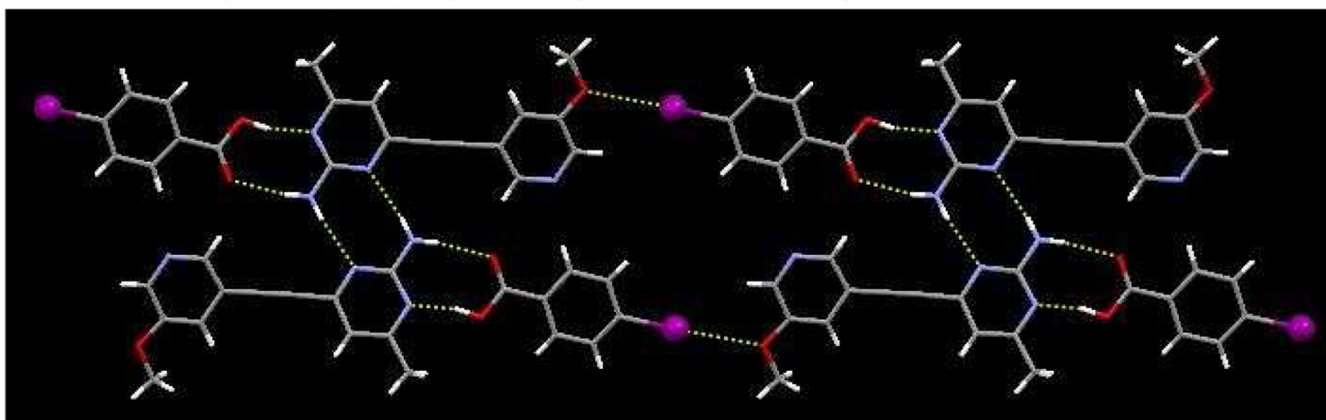


Figure 8. Ladder-type motif in the crystal structure of **3a** generated through combinations of hydrogen bonds and O...I halogen bonds.

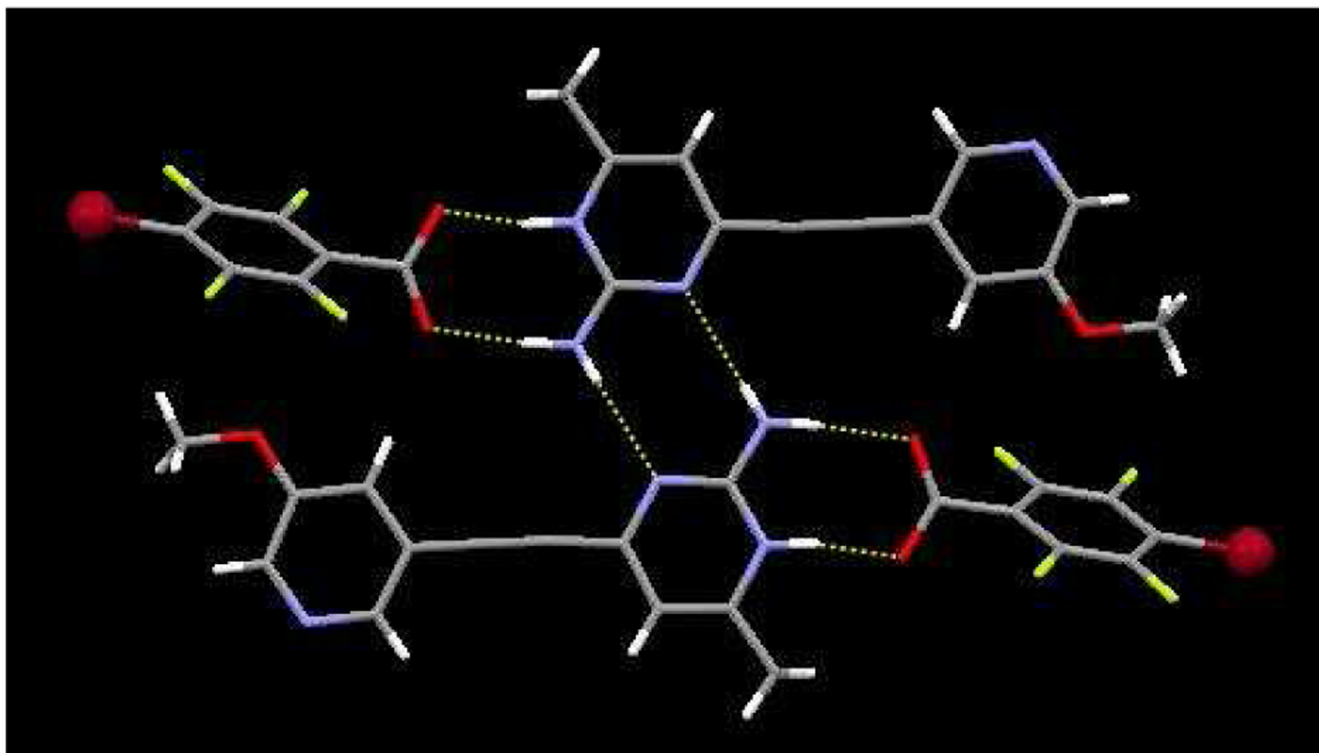
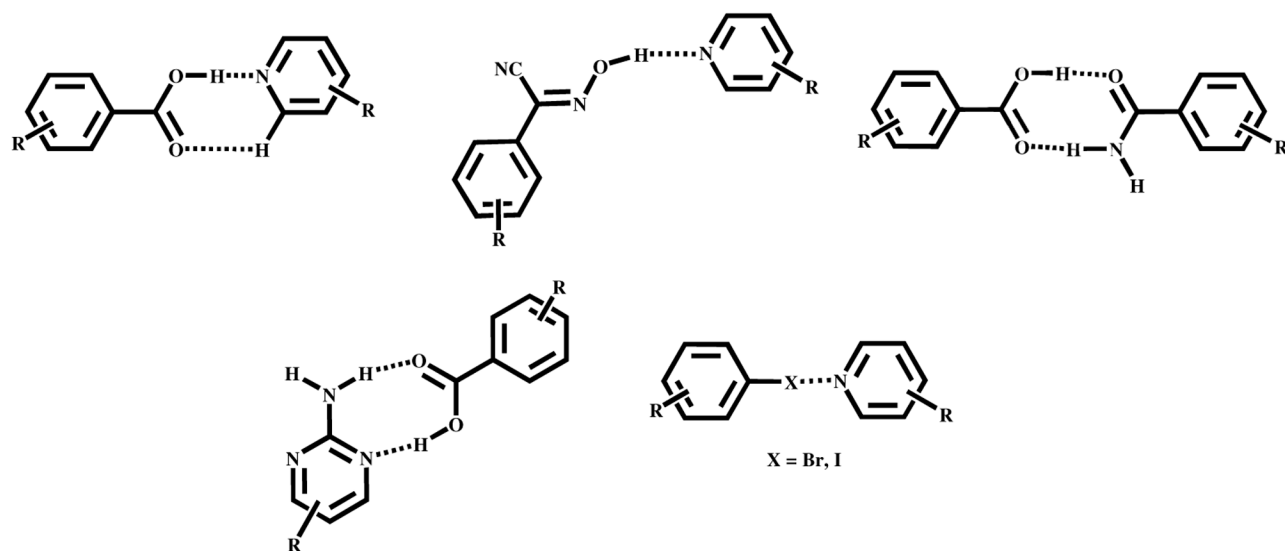
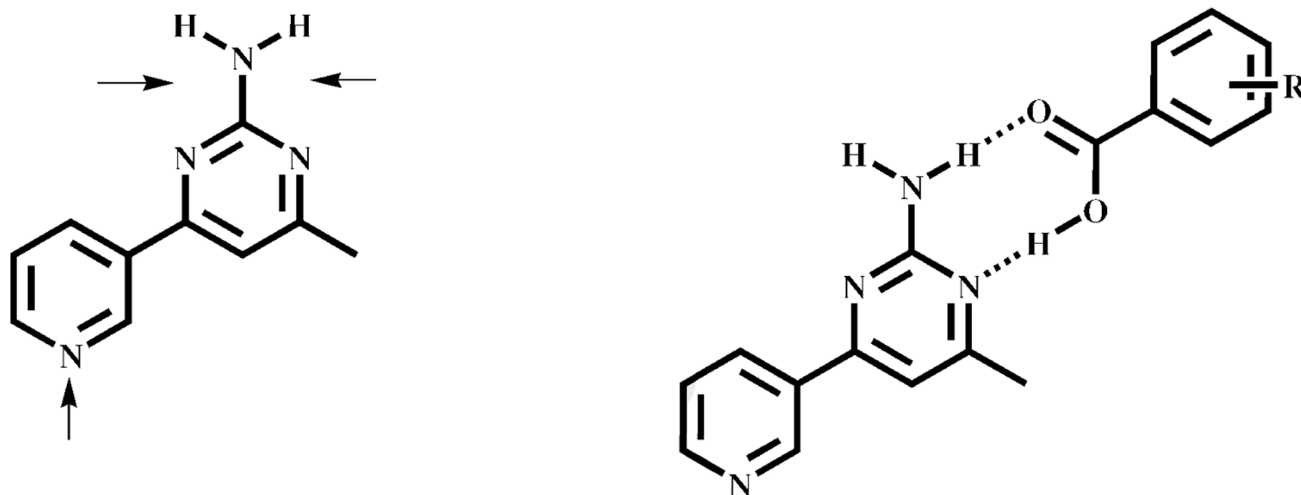


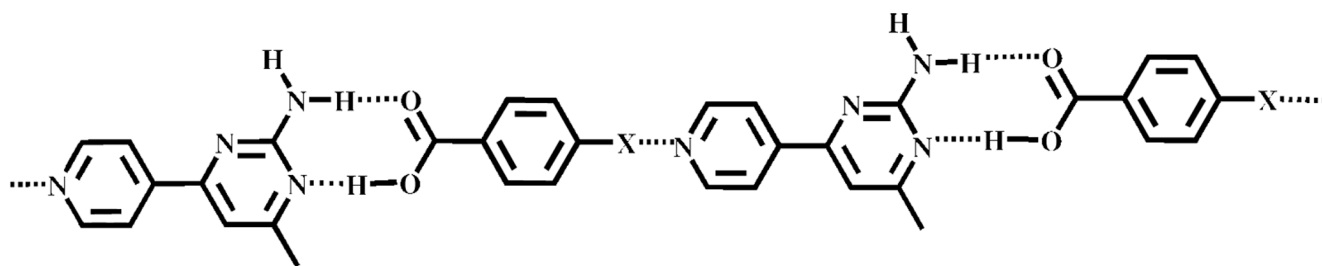
Figure 9. Supramolecular tetramer in **3b** formed *via* N-H \cdots O and N-H \cdots N hydrogen bonds.

**Scheme 1.**

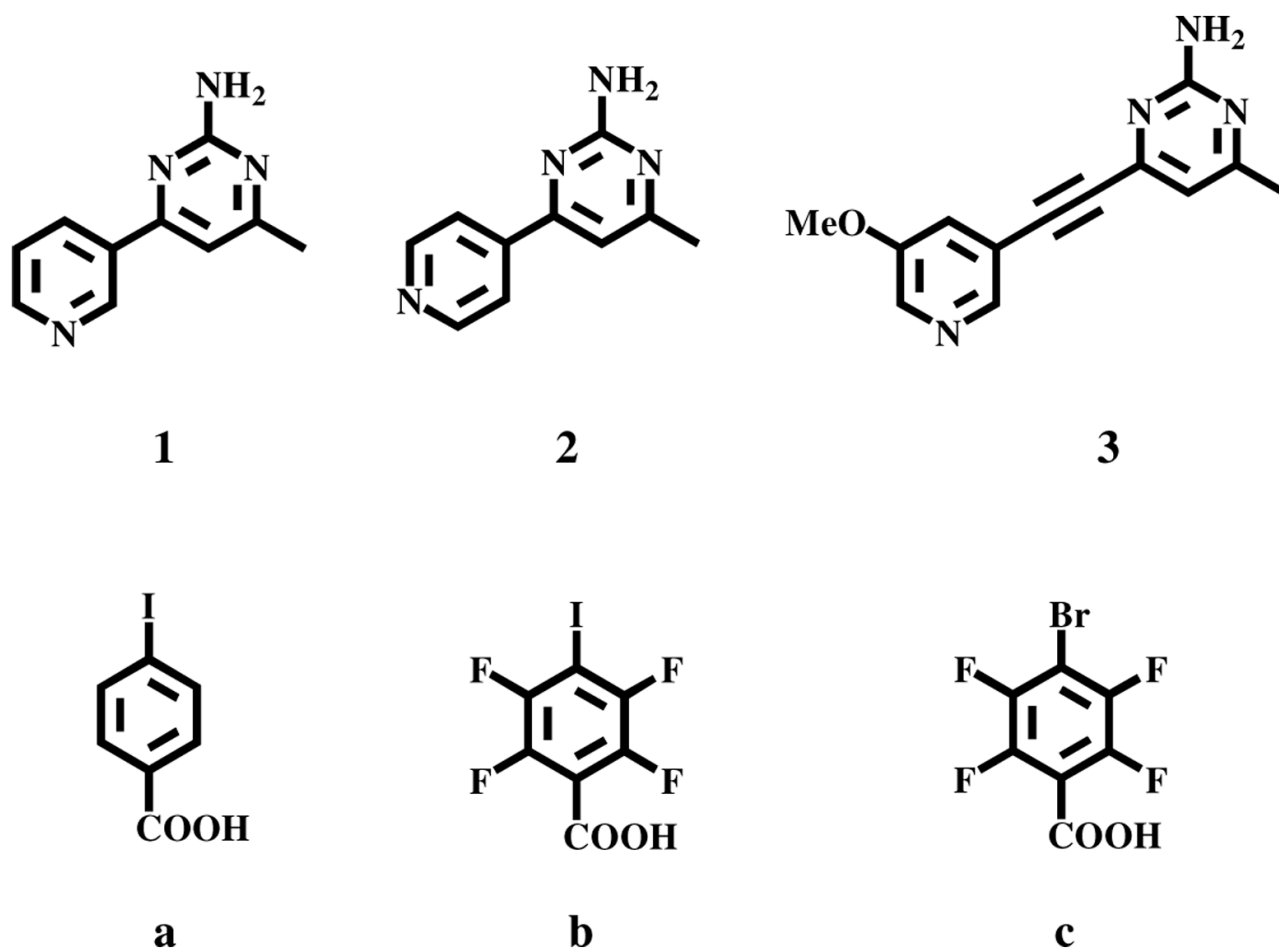
A few examples of heteromeric hydrogen-bond and halogen-bond based synthons.

**Scheme 2.**

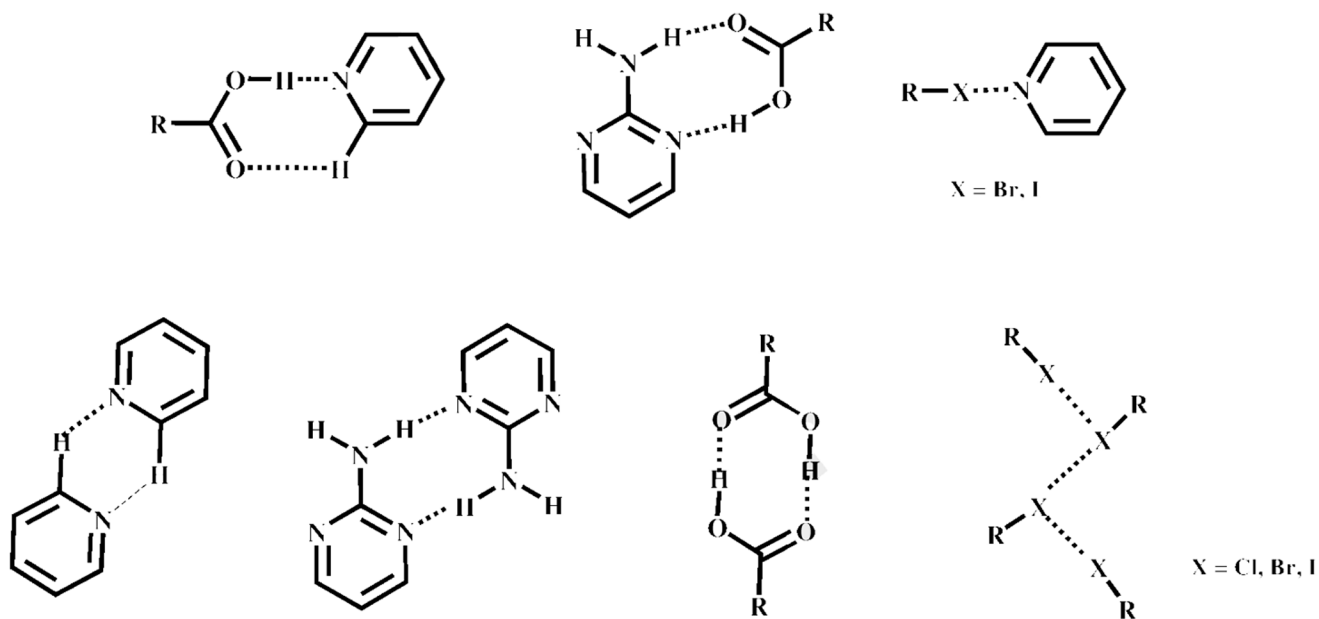
The three potential hydrogen-bonding sites on a pyridine/amino-pyrimidine (py/pym) SR (left). In 9/10 cases, the acid binds to an amino-pyrimidine site in preference to the pyridine moiety.

**Scheme 3.**

Supramolecular target constructed from hydrogen bonds and halogen bonds (X = I or Br).

**Scheme 4.**

Three bifunctional SR's, **1–3**, each possessing two distinctly different hydrogen-bonding moieties, py and amino-pym, and three halogenated aromatic carboxylic acids, **a–c**.

**Scheme 5.**

Potential heteromeric and/or homomeric synthons that could form between SR's **1–3** and halogenated benzoic acids **a–c**. The R group constitutes an aromatic ring.

Table 1

Crystallographic data for **1a–1b**, **2a–2c**, **3a**, and **3c**.

	1a	1b	2a	2b	2c	3a	3c
Empirical formula	C ₄₁ H ₃₈ I ₂ N ₈ O ₄	C ₁₇ H ₁₁ F ₄ IN ₄ O ₂	C ₁₇ H ₁₃ IN ₄ O ₂	C ₁₇ H ₁₁ F ₄ IN ₄ O ₂	C ₁₇ H ₁₁ F ₄ BrN ₄ O ₂	C ₂₀ H ₁₇ IN ₄ O ₃	C ₂₀ H ₁₃ BrF ₄ N ₄ O ₃
MW	960.59	506.20	434.23	506.20	459.21	488.28	513.25
Color, Habit	colorless block	pink plate	colorless, block	colorless, needle	colorless, prism	colorless, needle	colorless, plate
Crystal system	Triclinic	Monoclinic	Triclinic	Monoclinic	Monoclinic	Triclinic	Triclinic
Space group, Z	P-1, 1	P2(1)/n, 4	P-1, 2	P2(1)/c, 4	P2(1)/c, 4	P-1, 2	P-1, 2
a, Å	6.5689(2)	6.6313(15)	7.9304(7)	3.9153(4)	3.78950(10)	6.7820(5)	6.8878(2)
b, Å	9.5508(4)	34.494(8)	10.0937(9)	24.016(2)	24.2190(7)	8.9813(7)	7.4613(2)
c, Å	16.4413(6)	7.6535(18)	11.1149(10)	18.1909(15)	18.1436(5)	16.6932(11)	19.6275(7)
α, °	102.542(2)	90.00	109.850(3)	90	90	103.905(4)	80.331(2)
β, °	99.117(2)	103.151(16)	96.640(4)	92.995(4)	93.6890(10)	95.254(4)	88.064(2)
γ, °	96.534(2)	90.00	96.096(4)	90	90	100.313(5)	77.591(2)
Volume, Å ³	982.34(6)	1704.8(7)	821.10(13)	1708.1(2)	1665.68(8)	961.37(12)	971.13(5)
Density, g/cm ³	1.624	1.972	1.756	1.968	1.831	1.687	1.755
Temperature, K	293(2)	173(2)	153(2)	153(2)	293(2)	293(2)	293(2)
X-ray wavelength	0.71073	0.71073	0.71073	0.71073	0.71073	0.71073	0.71073
μ mm ⁻¹	1.653	1.943	1.968	1.939	1.939	1.695	2.187
θ min, °	3.18	1.18	1.97	2.78	3.36	2.39	2.11
θ max, °	27.50	28.76	27.48	27.13	27.12	27.62	27.10
Reflections							
collected	38388	12690	25406	40104	42293	39877	24991
independent	4495	4007	3768	3737	3662	4426	4292
observed	4183	2586	3473	2924	3227	3039	3946
Threshold expression	>2σ(I)	>2σ(I)	>2σ(I)	>2σ(I)	>2σ(I)	>2σ(I)	>2σ(I)
R ₁ (observed)	0.0217	0.0664	0.0360	0.0433	0.0243	0.0745	0.0246
wR ₂ (all)	0.0536	0.1768	0.0966	0.1189	0.0655	0.1928	0.0968

Table 2

Hydrogen-bond geometries for **1a–1b**, **2a–2c**, **3a**, and **3c**.

Structure	D-H...A	d(D-H)/Å	d(H...A)/Å	d(D...A)/Å	<(DHA) ^p
1a ^d	O(31)-H(31)...N(11)	0.98(2)	1.59(3)	2.5607(19)	168(2)
	N(12)-H(12A)...O(32)	0.84(2)	2.21(2)	3.035(2)	168(2)
	N(12)-H(12B)...N(21)#1	0.83(2)	2.12(2)	2.951(2)	177(2)
1b ^b	O(31)-H(31)...N(11)	0.84	1.77	2.589(7)	165.0
	N(12)-H(12A)...O(32)	0.88	2.06	2.924(8)	168.6
2a	N(12)-H(12B)...O(32)#1	0.88	2.05	2.855(8)	150.9
	N(11)-H(12A)...O(32)	0.88	1.95	2.818(4)	167.9
	O(31)-H(31)...N(11)	0.84	1.84	2.675(3)	172.6
2b ^c	N(11)-H(11)...O(31)	0.85(6)	1.81(6)	2.646(5)	167(5)
	N(12)-H(12A)...O(32)	0.88	1.94	2.801(5)	164.7
2c ^d	N(12)-H(12B)...O(32)#1	0.88	2.07	2.808(5)	141.4
	N(11)-H(11)...O(31)	0.82(2)	1.83(2)	2.6430(19)	173(2)
	N(12)-H(12A)...O(32)	0.84(2)	1.99(2)	2.823(2)	172(2)
3a ^e	N(12)-H(12B)...O(32)#1	0.89(2)	2.07(2)	2.812(2)	140(2)
	O(31)-H(31)...N(11)	0.97(9)	1.71(9)	2.643(8)	162(7)
	N(12)-H(12A)...O(32)	0.86	2.14	2.987(8)	169.3
3c ^f	N(12)-H(12B)...N(13)#1	0.86	2.28	3.108(8)	160.3
	N(11)-H(11)...O(31)	0.94(3)	1.68(3)	2.605(2)	169(2)
	N(12)-H(12A)...O(32)	0.93(3)	1.90(3)	2.832(2)	173(2)
	N(12)-H(12B)...N(13)#1	0.74(3)	2.34(3)	3.073(2)	170(3)

^a #1 -x, -y+2, -z+1

^b #1 -x+2, -y+1, -z+2

^c #1 -x+1, -y+1, -z+1

^d #1 -x+1, -y+2, -z+2

^e #1 -x, -y+1, -z

^f #1 -x+1, -y, -z+1

Table 3

Halogen bonds in crystal structures **1a–1b**, **2a–2c**, **3a**, and **3c**.

SR	Acid ^a	Structure #	Halogen bonds	Type of Halogen bond	Halogen bond Distance (Å)	C-X...N (°)
1	I-BA	1a	No	----	----	----
1	I-F ₄ BA	1b	Yes	I...N	2.941	170.7
2	I-BA	2a	Yes	I...N	3.004	177.1
2	I-F ₄ BA	2b	Yes	I...N	2.812	178.1
2	Br-F ₄ BA	2c	Yes	Br...N	2.840	177.6
3	I-BA	3a	Yes	I...O	3.265	178.1
3	Br-F ₄ BA	3c	No	----	----	----

^a I-BA = 4-iodobenzoic acid, I-F₄BA = 2,3,5,6-tetrafluoro-4-iodobenzoic acid, and Br-F₄BA = 2,3,5,6-tetrafluoro-4-bromobenzoic acid.

Table 4

Reported crystal structures containing short Br \cdots N and I \cdots N halogen bonds.

	Hits	N \cdots X distance (mean)	N \cdots X-C angle (mean)
Br \cdots N	29	3.28 Å	163 °
Br \cdots N (fluorinated)	11	2.95 Å	173 °
I \cdots N	21	3.17 Å	171 °
I \cdots N (fluorinated)	41	2.90 Å	173 °